Imaginary parts of coupled electron and phonon propagators

K. Schwartzman*
Department of Physics and Astronomy, Bates College, Lewiston, Maine 04240

W. E. Lawrence
Department of Physics and Astronomy, Dartmouth College, Hanover, New Hampshire 03755
(Received 31 July 1987)

Quasiparticle and phonon damping rates due to the electron-phonon and Coulomb interactions are obtained directly from the self-energy formalism of strong-coupling theory. This accounts for all processes involving phonon or quasiparticle decay into a single particle-hole pair, or quasiparticle decay by emission or absorption of a single real phonon. The two quasiparticle decay modes are treated on a common footing, without *ad hoc* separation, by accounting fully for the dynamics of the phonon propagator and the Coulomb vertex—the latter by expansion of the four-point Coulomb vertex function. The results are shown to be expressible in terms of only the physical (i.e., fully renormalized) energies and coupling constants, and are written in terms of spectral functions such as $\alpha^2F(\omega)$ and its generalizations. Expansion of these in powers of a phonon linewidth parameter distinguishes (in lowest orders) between quasiparticle decay modes involving real and virtual phonons. However, the simplest prescription for calculating decay rates involves an effective scattering amplitude in which this distinction is not made.

I. INTRODUCTION

The coupled Dyson's equations which are universally applied to the electron-phonon system were established by Migdal.[1] Migdal's equations are defined by the electron and phonon self-energies of Figs. 1(b) and 1(d), respectively, that are to be substituted into the general form of Dyson's equations

$$G = G^0(1+\Sigma G)\ , \tag{1a}$$

$$D = D^0(1+\Phi D)\ . \tag{1b}$$

Solid and wavy lines represent the full (i.e., self-consistently determined) electron and phonon propagators G and D, respectively. The same formal structure applies in the superconducting phase,[2] leading to coupled integral equations[3,4] which form the basis for calculations of superconducting phenomena under quite general circumstances including strong coupling, where the quasiparticle spectral distributions are not narrow. Coulomb interactions are included by Fig. 1(a) and by the dressing of electron-phonon vertices as indicated in Figs. 1(b)–1(d),[4,5] as will be discussed shortly.

The energies of quasiparticles and phonons are always of interest, and sometimes the decay rates are as well.

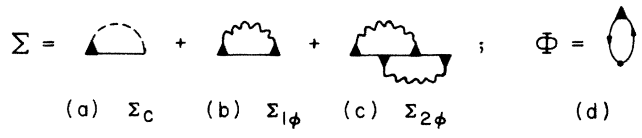

FIG. 1. Electron and phonon self-energies Σ and Φ. The electron self-energy is the sum of Coulomb, one-phonon, and two-phonon contributions, (a)–(c), respectively.

Some of the decay mechanisms stemming from the electron-phonon interaction are treated more or less naturally using the same self-energy-based formalism (e.g., the emission and absorption of real phonons by quasiparticles, and the decay of phonons into quasiparticle-hole pairs) as is discussed in Ref. 6. However, the decay of quasiparticle states into particle-hole pairs, via the Coulomb interaction or virtual-phonon mediation, have most often been discussed by appealing to other formalisms.[7,8] On the other hand, Migdal[1] showed that part of the phonon-mediated electron-electron mechanism is expressed through the phonon linewidth in the electron self-energy diagram, Fig. 1(b). This point was also mentioned by Holstein[9] and discussed in detail by Allen and Silberglitt.[10] Lopes dos Santos and Sherrington[11] showed more recently that the exchange analog of this contribution comes from an additional diagram, Fig. 1(c), previously excluded on the grounds of Migdal's theorem, which applies to $\mathrm{Re}\Sigma$, but which Ref. 11 generalizes for $\mathrm{Im}\Sigma$. The same authors later included the Coulomb interaction,[12] generalizing to finite temperatures an argument of Langer[13] in which $\mathrm{Im}\Sigma$ contributions are usefully classified according to decay modes of the initial state. Langer's ideas form the basis of the present derivations as well, although these differ from those of Refs. 11 and 12 in that, at the expense of elegance, each diagram of Fig. 1 is evaluated individually, maintaining the closest possible reference throughout to the physical phonon propagators and Coulomb vertices.

The primary purpose of this work is to show how all contributions to the inelastic decay rate τ^{-1} mentioned above may be obtained directly from the electron and phonon self-energies of conventional strong-coupling theory, with the addition of the single diagram as dictat-

ed by Ref. 11. This has the virtue of treating all important contributions to τ^{-1} on equal footing with each other, as well as with the real parts of the self-energies in terms of which renormalization and coupling parameters are expressed. In particular, following Allen and Silberglitt,[10] there is no *a priori* distinction between processes involving real and virtual phonons; such a distinction emerges naturally when linewidths are sufficiently narrow that distinct, approximately additive contributions to τ^{-1} may be identified. Furthermore, it is shown that the imaginary parts of Σ and Φ, unlike the real parts, can be written in terms of only the physical three- and four-point vertex functions; this, to our knowledge, has not been demonstrated previously. All contributions are expressed in terms of spectral functions associated with the decay products. In the present work, for clarity, attention is confined to the normal phase. The same approach is useful in studies of the superconducting phase,[14] which will be reported in detail in a future publication.

To be more specific about the relation between the imaginary parts of the self-energies and "physical" parameters, assume that the real parts of the self-energies (and particularly the quasiparticle and phonon energies) are known; it does not matter whether this knowledge comes from first-principles calculations, or by fits to experimental data. The decay rates are related to the imaginary parts, as illustrated by the simple expressions that apply to long-lived excitations: The quasiparticle energy ε_k and damping rate $\Gamma_k = 1/2\tau_k$ are given by

$$[G^0(\mathbf{k},\varepsilon_k)]^{-1} - \mathrm{Re}\Sigma(\mathbf{k},\varepsilon_k) = 0 \,, \tag{2a}$$

$$\Gamma_k = Z(\mathbf{k})^{-1}\mathrm{Im}\Sigma(\mathbf{k},\varepsilon_k) \,, \tag{2b}$$

$$Z(\mathbf{k}) = 1 - \partial[\mathrm{Re}\Sigma(\mathbf{k},\omega)]/\partial\omega \,|_{\omega=\varepsilon_k} \,, \tag{2c}$$

and the phonon quantities by

$$[D^0_\sigma(\mathbf{q},\omega_{q\sigma})]^{-1} - \mathrm{Re}\Phi_\sigma(\mathbf{q},\omega_{q\sigma}) = 0 \,, \tag{3a}$$

$$\gamma_{q\sigma} = \mathrm{Im}\Phi_\sigma(\mathbf{q},\omega_{q\sigma}) \,. \tag{3b}$$

With regard to coupling constants, the organizing element in this treatment is the Coulomb vertex (the solid triangles in Fig. 1). This vertex Λ contains screening as well as the proper Coulomb corrections, so that the dashed line in Fig. 1(a) is a bare Coulomb interaction. Aside from its role in Fig. 1(a), Λ serves in all the other diagrams to define the physical electron-phonon vertex g in terms of the bare vertex g^0 through

$$\begin{aligned} g_\sigma(K,Q) &= \Lambda(K,Q) g^0_\sigma(K,Q) \\ &= \sum_P [\delta_{PK} - 2k_B T \Gamma(K,P,Q) G(P+\tfrac{1}{2}Q) \\ &\quad \times G(P-\tfrac{1}{2}Q)] g^0_\sigma(P,Q) \,. \end{aligned} \tag{4}$$

The first equality states that g is both screened and (properly) Coulomb corrected, and the second equality expresses g (or Λ) in terms of the physical four-point vertex function Γ. It is implicit that Γ, like Λ, contains no phonon lines. The relationship between g and Γ is illustrated in Fig. 2. Upper-case arguments include for conciseness both the three-momentum and Matsubara frequency, i.e. $K = (\mathbf{k}, i\omega_n)$, and such arguments are assigned as specified by Fig. 2. (The modest level of complexity and the wish to exploit similarities to Lopes dos Santos and Sherrington's work[11] favors the use of the Matsubara formalism, although a direct real-time approach[15] is available.) With the help of Eq. (4), the imaginary parts of the analytically continued self-energies will eventually be written as Fermi-surface or Brillouin-zone integrals involving only the physical vertices g and Γ, with "unobservable" quantities such as g^0 and the bare Coulomb interaction eliminated. It should be noted for practical purposes that g may be accurately known in a particular case because it can be related to empirically determined electron-ion interaction parameters,[16] whereas Λ and Γ will not, in fact, be well known. In metals that superconduct, the phonon contributions may dominate the Coulomb ones (in some cases considerably) so that ignorance of the Coulomb vertices themselves may not seriously compromise the accuracy of computed decay rates.

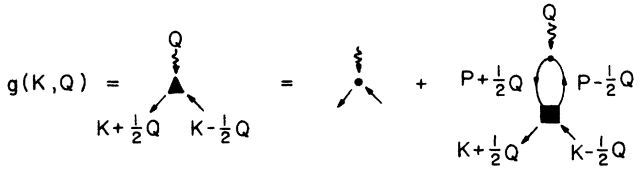

FIG. 2. Graphical illustration of Eq. (4): The dot represents the bare electron-phonon vertex g^0. The full electron-phonon vertex g is represented by a solid triangle when this is attached to a phonon line.

II. IMAGINARY PARTS

In this section, the imaginary part of each diagram in Fig. 1 is expressed in terms of spectral functions associated with the decay products. In the next section, detailed interpretations are made with the help of asymptotic expressions and a simple model. General results are reviewed in the final section, and a simple prescription given for calculating spectral functions and decay rates.

To begin with, it is important to note that the dynami-

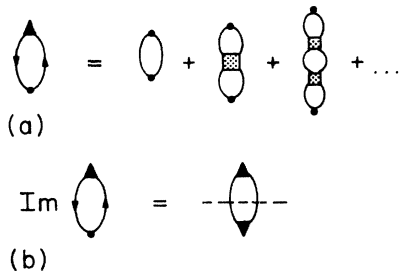

FIG. 3. (a) Expansion of the phonon self-energy using the Bethe-Salpeter equation. (b) Imaginary part of the analytically continued self-energy; dashed line indicates the contribution from a single particle-hole pair.

cal aspect of the Coulomb vertex is essential for all diagrams of Fig. 1 except for (c). Without it, there would be no Coulomb contribution to $\mathrm{Im}\Sigma$ (neither pure Coulomb nor interference between Coulomb and virtual-phonon mediation), and the phonon decay rate expression would display an unphysical asymmetry between bare and renormalized coupling constants. This vertex, therefore, will be the focus of early discussion.

Consider first the simplest case, namely the phonon self-energy of Fig. 1(d). Using the general relation between the three-point and four-point vertices g and Γ depicted in Fig. 2, and expanding Γ in irreducible elements via the Bethe-Salpeter equation,[17] Φ may be expressed as shown in Fig. 3(a). The expansion is made in the particle-hole channel that (by definition) exposes all particle-hole pairs which, if cut, break the diagram into two *vertex* parts. The summation of the results obtained by cutting all of the explicit particle-hole pairs may be represented by Fig. 3(b),[18] where a *full* Coulomb vertex is recovered on each side. The right-hand side is defined as that contribution to the imaginary part arising from the (explicit) particle-hole pair cut by the dashed line. This and other diagrams with dashed lines have no physical significance except as imaginary parts of analytically continued expressions. In this case the imaginary part provides the rate of phonon decay [Eq. (3b)] into single particle-hole pairs. In order to evaluate Fig. 3(b), consider the contribution $\delta\Phi(\mathbf{q},i\omega_m)$ of a single diagram in Fig. 3(a) in which the frequency sum associated with the chosen pair of lines to be cut is written explicitly,

$$\delta\Phi(Q)=-2k_BT\sum_K \delta g(K,Q)G(K+\tfrac{1}{2}Q)G(K-\tfrac{1}{2}Q)\delta g'(K,-Q)$$

$$=-2k_BT\sum_k\sum_n \delta g(K,Q)\delta g'(K,-Q)\int\int_{-\infty}^{\infty}\frac{d\varepsilon\,d\varepsilon'}{(2\pi)^2}\frac{\rho(\mathbf{k}+\mathbf{q}/2,\varepsilon)\rho(\mathbf{k}-\mathbf{q}/2,\varepsilon')}{\left[i\omega_n+\frac{i}{2}\omega_m-\varepsilon\right]\left[i\omega_n-\frac{i}{2}\omega_m-\varepsilon'\right]}\,, \tag{5}$$

where spectral representations of the electron Green's functions have been introduced, and $K=(\mathbf{k},i\omega_n)$. The vertex parts δg and $\delta g'$ pertain to the diagram and the cut chosen. The frequency sum is done by contour integration, and contributions arise not only from the two explicit poles, but also from poles occurring in the spectral representations of the adjoining irreducible four-point functions (which depend on ω_n). However, the latter poles correspond to final states involving more than a single particle-hole pair (by definition of the irreducible four-point function), and by Langer's argument generalized to finite temperatures[12] they contribute negligibly to the imaginary part of the analytically continued Φ. Therefore, keeping only those residues corresponding to the two explicit poles, one finds

$$\mathrm{Im}\Phi_{\sigma\sigma'}(\mathbf{q},\omega-i\eta)=2\sum_k g_\sigma(\mathbf{k},\mathbf{q})P(\mathbf{k},\mathbf{q},\omega)g_{\sigma'}(\mathbf{k},\mathbf{q})\,, \tag{6}$$

where all contributions of the type written in Eq. (5) have been summed, and full vertices are collected on both sides of the cut, as shown in Fig. 3(b).[18] Since imaginary part contributions have been isolated in the factor P, the vertex functions are understood to be real. As a result, they are also essentially frequency independent,[19] as implied by dropping the frequency arguments.

The other step leading from Eq. (5) to Eq. (6) (i.e., taking the imaginary part of the analytically continued $i\omega_m\to\Omega-i\eta$ frequency sum) defines the spectral density of a particle-hole pair with constituent momenta $\mathbf{k}\pm\mathbf{q}/2$;

$$P(\mathbf{k},\mathbf{q},\omega)=\int_{-\infty}^{\infty}\frac{d\varepsilon}{4\pi}[f(\varepsilon)-f(\varepsilon+\omega)]\rho(\mathbf{k}-\tfrac{1}{2}\mathbf{q},\varepsilon)$$

$$\times\rho(\mathbf{k}+\tfrac{1}{2}\mathbf{q},\varepsilon+\omega) \tag{7a}$$

$$\approx\pi\omega\delta(\varepsilon_{k-(1/2)q})\delta(\varepsilon_{k+(1/2)q})$$

$$\times[Z(\mathbf{k}-\tfrac{1}{2}\mathbf{q})Z(\mathbf{k}+\tfrac{1}{2}\mathbf{q})]^{-1}\,. \tag{7b}$$

The second equality expresses the fact that the product $\rho\rho$ serves only to restrict the $\mathbf{k}$ integral to the region where both $\mathbf{k}\pm\mathbf{q}/2$ are near the Fermi surface;[20] it does not introduce a dependence on quasiparticle width,[11] or otherwise alter the linear ω dependence of P,[20] which arises from the difference of Fermi functions. Hence these functions may be evaluated at zero width, $\rho(\mathbf{k},\varepsilon)\to 2\pi Z^{-1}(\mathbf{k})\delta(\varepsilon_k)=2\pi\delta(Z\varepsilon_k)$, where $Z(\mathbf{k})$ is the quasiparticle renormalization factor in Eq. (2c).

It is useful to consider in a similar manner the vertex itself. The analogous procedure is to cut all particle-hole pairs that separate the phonon point from the particle and hole points. An expansion in irreducible four-point vertices similar to that of Fig. 3(a), followed by a summation over all ways of cutting single explicit particle-hole pairs, gives rise to Fig. 4, in which the full three- and four-point vertices appear. The algebraic expression is easily derived by comparison with the previous case, and the analog of Eq. (6) is

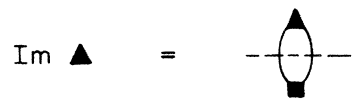

FIG. 4. Graphical representation of Eq. (8) for the imaginary part of the analytically continued electron-phonon vertex.

$$\mathrm{Im}g_\sigma(\mathbf{k},\mathbf{q},\omega-i\eta)=\sum_p \Gamma(\mathbf{k},\mathbf{p},\mathbf{q})P(\mathbf{p},\mathbf{q},\omega)g_\sigma(\mathbf{p},\mathbf{q}) , \quad (8)$$

where the product ΓP implies spin summation (since Γ is spin dependent), unlike Eq. (6) where the spin sum trivially produces the factor 2. The imaginary part of the vertex does not by itself represent a physical quantity. However, the foregoing arguments suggest a means of treating the vertex when it appears as part of a larger diagram whose imaginary part is interesting.

In the single-phonon graph [Fig. 1(b)], the imaginary part is dominated by final states that differ from the initial quasiparticle state by a single phonon or a single particle-hole pair. Accordingly, consider cuts which involve the explicit particle line, together with either the phonon propagator or one of the vertices. It suffices to cut the vertices in the manner leading to Eq. (8), so that the nature of the result may be anticipated by Fig. 5, as will be confirmed in the following analysis.

To find the algebraic expression for the contributions $\mathrm{Im}\Sigma_{1\phi}$ [(i) and (iii) in Fig. 5(a)] in which a vertex is cut, one may sum the independent internal frequency variable of the particle-hole pair as in deriving Eq. (8), but one cannot analytically continue the vertex by itself. Instead, the vertex frequency variable ω_m must be summed in the expression

$$\Sigma_{1\phi}(K)=-k_BT\sum_Q G(K-Q)g_\sigma(K-\tfrac{1}{2}Q,Q) \times D_{\sigma\sigma'}(Q)g_{\sigma'}(K-\tfrac{1}{2}Q,-Q) , \quad (9)$$

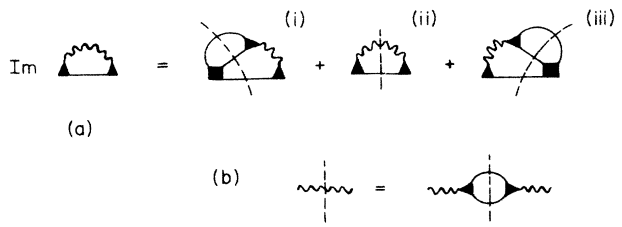

FIG. 5. (a) Imaginary part of the analytically continued electron self-energy term $\Sigma_{1\phi}$, showing contributions (i) and (iii) from the vertices, and (ii) from the phonon propagator. (b) Imaginary part of the analytically continued phonon propagator.

where $Q=(\mathbf{q},i\omega_m)$, and the important dependence on ω_m occurs in the propagators G and electron-phonon vertices g_σ to be cut. To make this dependence explicit, G is written in spectral representation (introducing the frequency denominator $i\omega_n-i\omega_m-\varepsilon$), and Eq. (8) is written as it would appear prior to analytic continuation,

$$g_\sigma^{\mathrm{eff}}(\mathbf{k}-\mathbf{q}/2,\mathbf{q},i\omega_m) = \sum_p \Gamma(\mathbf{k}-\tfrac{1}{2}\mathbf{q},\mathbf{p},\mathbf{q}) \times\int_{-\infty}^{\infty}\frac{d\omega}{\pi}P(\mathbf{p},\mathbf{q},\omega)(i\omega_m-\omega)^{-1}g_\sigma(\mathbf{p},\mathbf{q}) . \quad (10)$$

The notation g^{eff} means that Eq. (10) is valid only if the vertex is going to be cut; otherwise, the internal frequency variable of the particle-hole pair cannot be decoupled from the adjoining vertex functions. The resulting frequency sum $\sum_m(i\omega_n-i\omega_m-\varepsilon)^{-1}(i\omega_m-\omega)^{-1}$ may be done, and this result analytically continued to give

$$\mathrm{Im}\Sigma_{1\phi}^{(\mathrm{i})}(\mathbf{k},\varepsilon-i\eta)=\sum_q\sum_p\int_{-\infty}^{\infty}\frac{d\omega}{2\pi}\rho(\mathbf{k}-\mathbf{q},\varepsilon-\omega)\Gamma(\mathbf{k}-\tfrac{1}{2}\mathbf{q},\mathbf{p},\mathbf{q})P(\mathbf{p},\mathbf{q},\omega)[n(\omega)+1-f(\varepsilon-\omega)] \times g_\sigma(\mathbf{p},\mathbf{q})\mathrm{Re}D_\sigma(\mathbf{q},\omega)g_\sigma(\mathbf{k}-\tfrac{1}{2}\mathbf{q},\mathbf{q}) \quad (11)$$

[where the designation (i) refers to Fig. 5(a)]. The real part of $D_\sigma(\mathbf{q},\omega)$ is taken for the same reason that the real parts of g and Γ are taken in Eqs. (6) and (8), for example, as well as in Eq. (11); these represent elements in which no lines are cut. In the expressions referred to, it is the spectral density P that arises from the cut G lines. Of course the frequency dependence of $\mathrm{Re}D_\sigma$ cannot be ignored (unlike that of the real parts of the vertices); a simplification that does occur is that $\mathrm{Re}D$ is diagonal in polarization σ, as is implicit in Eq. (3a).

The contribution from cutting the phonon line, $\mathrm{Im}\Sigma_{1\phi}^{(\mathrm{ii})}$, is seen from the spectral representation

$$D_{\sigma\sigma'}(\mathbf{q},i\omega_m)=\int_{-\infty}^{\infty}\frac{d\omega}{2\pi}B_{\sigma\sigma'}(\mathbf{q},\omega)(i\omega_m-\omega)^{-1} \quad (12)$$

to involve exactly the same occupation factors as Eq. (11), and this suggests that the common factor (containing all the T and ε dependence) be separated from the different spectral (i.e., ω-dependent) functions. As usual, the positive and negative ω domains may be combined using the oddness of $P(\omega)$ and $B(\omega)$, and the properties of Bose and Fermi functions n and f, so that

$$\mathrm{Im}\Sigma_{1\phi}(\mathbf{k},\varepsilon-i\eta)=\int_0^{\infty}d\omega[2n(\omega)+f(\omega-\varepsilon)+f(\omega+\varepsilon)]S_{1\phi}(\mathbf{k},\omega) . \quad (13)$$

As earlier, one may put $\rho(k-q,\varepsilon-\omega)\to 2\pi\delta(Z\varepsilon_{k-q})$, since this factor serves only to restrict the $\mathbf{q}$ integration so that $\mathbf{k}-\mathbf{q}$ is near the Fermi surface; it contributes

essentially no ε or ω dependence. Thus

$$S^{(i)}_{1\phi}(\mathbf{k},\omega)=S^{(iii)}_{1\phi}(\mathbf{k},\omega)$$
$$=\sum_q\sum_p \delta(Z\varepsilon_{k-q})\Gamma(\mathbf{k}-\tfrac{1}{2}\mathbf{q},\mathbf{p},\mathbf{q})$$
$$\times P(\mathbf{p},\mathbf{q},\omega)g_\sigma(\mathbf{p},\mathbf{q})\mathrm{Re}D_{\sigma\sigma'}(\mathbf{q},\omega)$$
$$\times g_{\sigma'}(\mathbf{k}-\tfrac{1}{2}\mathbf{q},\mathbf{q}) \quad (14)$$

and

$$S^{(ii)}_{1\phi}(\mathbf{k},\omega)=\sum_q \delta(Z\varepsilon_{k-q})g_\sigma(\mathbf{k}-\tfrac{1}{2}\mathbf{q},\mathbf{q})$$
$$\times\tfrac{1}{2}B_{\sigma\sigma'}(\mathbf{q},\omega)g_{\sigma'}(\mathbf{k}-\tfrac{1}{2}\mathbf{q},\mathbf{q})\ . \quad (15)$$

The ω dependences of the spectral functions $S_{1\phi}$ [(i) and (ii)] come mainly from $P(\omega)$ and $B(\omega)$. These differ near $\omega\sim\omega_q$, where B represents real phonons, but at much lower frequencies, B shares the linear dependence of P on ω, reflecting the particle-hole decay mode.[10] To see this explicitly it is useful to express $B_{\sigma\sigma'}$ in terms of $\mathrm{Im}\Phi_{\sigma\sigma'}$, and hence P.

First, it follows from Eq. (12) that

$$B_{\sigma\sigma'}(\mathbf{q},\omega)=2\,\mathrm{Im}D_{\sigma\sigma'}(\mathbf{q},\omega-i\eta)\ . \quad (16)$$

Now the *inverse* of the D matrix can be written concisely [Eq. (1b)] as

$$D^{-1}_{\sigma\sigma'}(\mathbf{q},\omega)=\delta_{\sigma\sigma'}(\omega^2-\omega^2_{q\sigma})/2\omega_{q\sigma}-i\,\mathrm{Im}\Phi_{\sigma\sigma'}(\mathbf{q},\omega)\ , \quad (17)$$

where $\mathrm{Re}\Phi_{\sigma\sigma'}$ has been diagonalized and absorbed into the physical frequencies $\omega_{q\sigma}$. However, the exact D matrix itself is unwieldy because $\mathrm{Im}\Phi_{\sigma\sigma'}$ has off-diagonal elements that are of the same order of magnitude [Eq. (6)] as the diagonal ones. Fortunately, only the leading terms of an expansion in powers of $\mathrm{Im}\Phi$ contribute significantly to $S_{1\phi}(\omega)$. Thus, to a good approximation, the B matrix is given by the following: Its diagonal elements are

$$B_{\sigma\sigma}(\mathbf{q},\omega)\cong 2\,|\,D_\sigma(\mathbf{q},\omega)\,|^2\mathrm{Im}\Phi_{\sigma\sigma}(\mathbf{q},\omega)\ , \quad (18a)$$

while for $\sigma'\neq\sigma$,

$$B_{\sigma\sigma'}(\mathbf{q},\omega)\cong 2\,\mathrm{Re}D_\sigma(\mathbf{q},\omega)\mathrm{Re}D_{\sigma'}(\mathbf{q},\omega)\mathrm{Im}\Phi_{\sigma\sigma'}(\mathbf{q},\omega)\ . \quad (18b)$$

The first expression is no different from the usual form used (for example, by Allen and Silberglitt[10]) when off-diagonal elements are of no concern. In both expressions, a single subscript (D_σ) refers to the usual definition of the phonon propagator as the inverse of a diagonal element of Eq. (17). The asymmetry between Eqs. (18a) and (18b) deserves brief comment here: The exact expression for $\sigma'\neq\sigma$ contains $-2\,\mathrm{Im}D_\sigma\mathrm{Im}D_{\sigma'}\mathrm{Im}\Phi$ and several other terms of the same order, namely $(\mathrm{Im}\Phi)^3$. These are dropped because they do not contribute significantly to $S_{1\phi}(\omega)$. The corresponding term in Eq. (18a), namely $2(\mathrm{Im}D_\sigma)^2\mathrm{Im}\Phi_{\sigma\sigma}$, is retained because although formally of order $(\mathrm{Im}\Phi)^3$, there is a contribution to $S_{1\phi}$ arising from the pole of D_σ (representing real-phonon processes) to which this term contributes equally with the $(\mathrm{Re}D_\sigma)^2\mathrm{Im}\Phi_{\sigma\sigma}$ term ($\mathrm{Re}D_\sigma$ has a zero near the pole of D_σ). All other terms in the expansion of $B_{\sigma\sigma}$ contribute less than these two terms by at least two powers of $\mathrm{Im}\Phi$. The $\sigma'\neq\sigma$ terms [Eq. (18b)] do not contribute significantly to the real-phonon component of $S_{1\phi}$ because the poles of D_σ and $D_{\sigma'}$ are separated by an amount large compared with $\mathrm{Im}\Phi$. Hence only the term which is formally first order in $\mathrm{Im}\Phi$ in fact contributes appreciably. The identification of electron-phonon versus electron-electron components of $S_{1\phi}(\omega)$ is based on asymptotic expansions in the phonon linewidth parameter (essentially $\mathrm{Im}\Phi$) carried out in the next section. The validity of the present arguments is most easily checked using those methods. If phonon linewidths are not much smaller than phonon frequency differences, then $D_{\sigma\sigma'}$ should be computed exactly for use in Eqs. (14)–(16). To conclude the present discussion, however, the contribution from $\sigma'\neq\sigma$ elements to $S^{(ii)}_{1\phi}$ is written by substituting Eq. (18b) into Eq. (15), with $\mathrm{Im}\Phi$ as given by Eq. (6):

$$S^{(ii)}_{1\phi}(\mathbf{k},\omega)\,|_{\sigma'\neq\sigma}\cong\sum_q\sum_{q'}\delta(Z\varepsilon_{k-q})g_\sigma(\mathbf{k}-\tfrac{1}{2}\mathbf{q},\mathbf{q})$$
$$\times\mathrm{Re}D_\sigma(\mathbf{q},\omega)g_\sigma(\mathbf{q}',\mathbf{q})$$
$$\times 2P(\mathbf{q}',\mathbf{q},\omega)g_{\sigma'}(\mathbf{q}',\mathbf{q})$$
$$\times\mathrm{Re}D_{\sigma'}(\mathbf{q},\omega)g_{\sigma'}(\mathbf{k}-\tfrac{1}{2}\mathbf{q},\mathbf{q})\ . \quad (19)$$

The analogy with Eq. (14) is now clearer. In particular, it is apparent from the foregoing discussion that the electron-electron contributions all arise from integrals involving only $\mathrm{Re}D_\sigma$ apart from a single power of $\mathrm{Im}\Phi$ or P that determines the low-ω behavior $S(\omega)\sim\omega$. This is a reflection of the fact that leading electron-electron behavior is obtained by cutting three G lines [two of which are always implicit in Figs. 1(a) and 1(b)]. Note in particular that Eq. (19) could be derived by an expansion of the phonon propagator, followed by a summation over all cuts which break a bubble so generated.

The purely Coulomb contribution $\mathrm{Im}\Sigma_c$ [Fig. 1(a)] may be computed as indicated by Fig. 6. The cut lines indicate two frequency sums which are identical to those done above, so that the temperature and energy dependences of $\mathrm{Im}\Sigma_c(\mathbf{k},\varepsilon-i\eta)$ are again described by Eq. (13), with a spectral function of the form of Eq. (14). In this

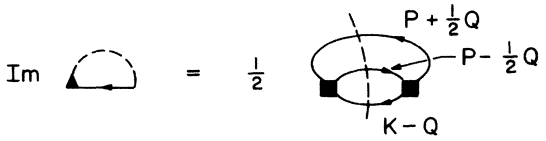

FIG. 6. Imaginary part of the analytically continued electron self-energy term Σ_c.

case the spin sum involves all three intermediate G lines rather than just two. Thus, if the external spin is up, there is one intermediate state in which all spins are up, but now two intermediate states in which a pair of spins is reversed. In the latter cases, the reversed spins may be identified with the particle-hole pair. Writing the spin sum explicitly, the spectral function corresponding to Σ_c is

$$S_c(\mathbf{k},\omega)=\tfrac{1}{2}\sum_q\sum_{q'}\delta(Z\varepsilon_{k-q})P(\mathbf{q}',\mathbf{q},\omega)\times[\Gamma^2_{\uparrow\uparrow}(\mathbf{k}-\tfrac{1}{2}\mathbf{q},\mathbf{q}',\mathbf{q})+2\Gamma^2_{\uparrow\downarrow}(\mathbf{k}-\tfrac{1}{2}\mathbf{q},\mathbf{q}',\mathbf{q})]\ . \tag{20}$$

The spin subscripts refer to the incoming spin states, i.e., to the spins of the external electron and the hole. This result is equivalent to Eq. (24) of Ref. 12. In a previous case, Eq. (14), in which one intermediate spin is constrained, the spin sum produces the factor $\Gamma_{\uparrow\uparrow}+\Gamma_{\uparrow\downarrow}$.

In the two-phonon graph [Fig. 1(c)], the only significant contributions to $\mathrm{Im}\Sigma_{2\phi}$ arise from cutting the three explicit particle lines.[11] One may examine other contributions arising when a phonon line is cut, as in Ref. 11, or when a vertex (i.e., an implicit particle-hole pair) is cut. In either case, one of the two pieces into which the diagram is broken contains a phonon correction to an electron-phonon vertex. Since the real part of this vertex appears in the final expression, its contribution to $\mathrm{Im}\Sigma_{2\phi}$ is negligible compared with $\mathrm{Im}\Sigma_{1\phi}$ and may be ignored. Proceeding to cut the three explicit particle lines, one can identify an effective particle-hole pair (in either of two ways) and express the two frequency sums in the same manner as before. Upon analytic continuation, one is again left with real parts of vertices and phonon propagators. This renders the vertices static and $\mathrm{Re}D_\sigma$ diagonal, but the two $\mathrm{Re}D$ factors remain frequency dependent. Because these depend upon the two independent internal frequencies, the result cannot in general be put in the form of Eq. (13), and so it is instead written

$$\mathrm{Im}\Sigma_{2\phi}(\mathbf{k},\varepsilon-i\eta)=\int_{-\infty}^{\infty}d\omega[n(\omega)+f(\omega-\varepsilon)]\times\int_{-\infty}^{\infty}d\omega'[f(\varepsilon-\omega'-\omega)-f(\varepsilon-\omega')]\times S_{2\phi}(\mathbf{k},\omega,\omega') \tag{21a}$$

with

$$S_{2\phi}(\mathbf{k},\omega,\omega')=-\pi\sum_q\sum_{q'}\delta(Z\varepsilon_{k-q})\delta(Z\varepsilon_{k-q'})\delta(Z\varepsilon_{k-q-q'})g_\sigma(\mathbf{k}-\tfrac{1}{2}\mathbf{q},\mathbf{q})\mathrm{Re}D_\sigma(\mathbf{q},\omega)g_\sigma(\mathbf{k}-\tfrac{1}{2}\mathbf{q}-\mathbf{q}',\mathbf{q})\times g_{\sigma'}(\mathbf{k}-\tfrac{1}{2}\mathbf{q}'-\mathbf{q},\mathbf{q}')\mathrm{Re}D_{\sigma'}(\mathbf{q}',\omega')g_{\sigma'}(\mathbf{k}-\tfrac{1}{2}\mathbf{q}',\mathbf{q}')\ . \tag{21b}$$

Note that all contributions to $\mathrm{Im}\Sigma$ may be put in the form of Eq. (21a), as is easily verified by inspection of Eqs. (11) and (7a) (in previous cases there was no need to, since the ω' integrals could be done immediately). In the present case the ω' integral may be done for ε and $T\ll\omega_D$, with the result that Eq. (21a) reduces to the form of Eq. (13) with an effective spectral function linear in ω for $\omega\ll\omega_D$. This is indicative of electron-electron scattering, and a comparison of Eq. (21b) with Eq. (19) identifies $\mathrm{Im}\Sigma_{2\phi}$ as the exchange counterpart of (the electron-electron part of) $\mathrm{Im}\Sigma^{(\mathrm{ii})}_{1\phi}$. The same comparison suggests (correctly) that Eq. (21b) does not contribute substantially to real-phonon processes; contributions from the poles of D_σ are of the same order as those found in $S^{(\mathrm{ii})}_{1\phi}$ for $\sigma'\neq\sigma$.

In summary, Figs. 1(a)–1(c) all contribute to the particle-hole pair production rate due to the Coulomb interaction and/or virtual-phonon mediation. Only the graph in Fig. 1(b), and only that contribution shown in Fig. 5(ii) with $\sigma'=\sigma$ contributes appreciably to the real-phonon emission or absorption rate by quasiparticles. The various contributions to $S(\omega)$ and $\mathrm{Im}\Sigma(\varepsilon,T)$ will be discussed more quantitatively in the next section.

III. INTERPRETATION

There is an intuitively appealing, if only heuristic way to organize the various contributions to $\mathrm{Im}\Sigma$ studied in the last section, and that is to consider the "effective" diagrams shown in Fig. 7. The electron and phonon propagators and the vertices are all physical ones. Figure 7(c) represents an exact parametrization of the static four-point vertex in the manifestly antisymmetric form[8]

$$\Gamma_{\uparrow\uparrow}(\mathbf{k},\mathbf{p},\mathbf{q})=V_{\uparrow\uparrow}(\mathbf{q})-V_{\uparrow\uparrow}(\mathbf{k}-\mathbf{p})\ , \tag{22a}$$

$$\Gamma_{\uparrow\downarrow}(\mathbf{k},\mathbf{p},\mathbf{q})=V_{\uparrow\downarrow}(\mathbf{q})\ , \tag{22b}$$

so that a dotted line represents $V_{\uparrow\uparrow}$ or $V_{\uparrow\downarrow}$ according to the particle lines it connects. The term "effective" means that these diagrams are not part of a rigorous perturbation expansion; in particular, the first diagram in Fig. 7(a) (polarization) is not a skeleton diagram, and would lead to redundancy with first-order diagrams [Figs. 1(a) and 1(b)] in a calculation of, say, $\mathrm{Re}\Sigma$. The point is that the diagrams of Fig. 7(a) may be used in *place* of those of Figs. 1(a)–1(c) in calculating $\mathrm{Im}\Sigma$, with the understanding that now only *explicit* G lines are to be cut. This implies that a factor of $\mathrm{Re}D_\sigma$ is to be associated with a phonon line upon analytic continuation. The prescription so far accounts for the full electron-electron contribution, but only half the electron-phonon one. To account completely for the latter, it is necessary to replace $(\mathrm{Re}D_\sigma)^2$ by $|D_\sigma|^2$ whenever two phonon lines with $\sigma'=\sigma$ appear in the polarization diagram. A simpler approximate prescription will be given in the

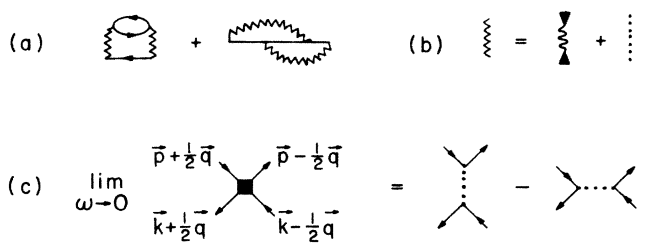

FIG. 7. Effective diagrams useful for interpreting the results of the last section; diagrams (a) provide contributions to ImΣ, (b) define the effective interaction potential, and (c) parametrize the static four-point Coulomb vertex.

final section, where a discussion of errors can be made using the results of this section.

A detailed correspondence between diagrams in Fig. 7 and Figs. 1(a)–1(c) may now be drawn by expanding Fig. 7(a) into eight separate diagrams. The two purely Coulomb ones correspond to Fig. 1(a), another corresponds to Fig. 1(c), and the remaining five to Fig. 1(b). Four of these five contain both a phonon line and a Coulomb line, and thus represent $S_{1\phi}$ [(i) and (iii)]. The remaining diagram represents $S_{1\phi}^{(ii)}$, and this is the only one which contributes non-negligibly to real-phonon processes, as discussed qualitatively in Sec. II.

The various contributions may be compared quantitatively by considering the asymptotic energy and temperature dependences of ImΣ, or better yet, the frequency dependences of the spectral functions $S(\omega)$. The asymptotic forms depend on the fact that the phonon self-energy, according to Eqs. (6) and (7), satisfies

$$\mathrm{Im}\Phi_{\sigma\sigma'}(\mathbf{q},\omega)=\alpha_{\sigma\sigma'}(\mathbf{q})\omega \ , \tag{23}$$

where the coefficient $\alpha_{\sigma\sigma'}(\mathbf{q})$ is a Fermi-surface integral of a product of vertex functions. For small $\mathbf{q}$, $g_\sigma \sim \sqrt{q}$ and hence $\alpha_{\sigma\sigma'}(\mathbf{q})$ approaches a constant. The discussion is simplified by the use of the Debye model (but allowing for different phonon polarizations), and the assumption of a spherical Fermi surface with electron effective mass m. The usual expressions are

$$\omega_{q\sigma}=c_\sigma q \ , \tag{24a}$$

$$g_\sigma(q)=b_\sigma\sqrt{q} \ . \tag{24b}$$

Using Eq. (24b) in Eqs. (6) and (7) then leads to

$$\alpha_{\sigma\sigma'}=\frac{m^2}{2\pi\hbar^3}b_\sigma b_{\sigma'} \ . \tag{25}$$

The effect of the model is simply to extend the small-$\mathbf{q}$ dependences to all $\mathbf{q}$, and to make these dependences isotropic. This allows the momentum integrations to be done analytically, resulting in simple expressions. More general (and cumbersome) results can be obtained without difficulty.

To begin with, note that Eq. (21b) expresses $S_{2\phi}$ as a double three-momentum integral subject to the constraint that the three variable quasiparticle momenta lie on the Fermi surface. All the other spectral functions are similarly expressed by Eqs. (14), (19), and (20), in which the factor P contains two of the three constraining δ functions [Eq. (7b)]. These three δ functions reduce the six independent momentum variables to three—the number required to specify the positions (on the Fermi surface) of three quasiparticles that can engage in momentum-conserving scattering events with the fixed state $\mathbf{k}$ (Fig. 8). Azimuthal symmetry of the integrand with respect to $\mathbf{k}$ allows reduction of this number to two—the magnitudes of momenta transferred in the direct and exchange terms. In the case of Eq. (21b), these are the two phonon wave-vector magnitudes q and q':

$$\sum_q\sum_{q'}\delta(Z\varepsilon_{k-q})\delta(Z\varepsilon_{k-q'})\delta(Z\varepsilon_{k-q-q'})=\frac{1}{\pi}\left[\frac{m}{2\pi\hbar^2}\right]^3\int\int dq\,dq'\frac{\Theta((2k_F)^2-q^2-(q')^2)}{\pi k_F[(2k_F)^2-q^2-(q')^2]^{1/2}} \ . \tag{26}$$

Using Eqs. (24b) and (25) for the vertex functions, Eq. (21b) reduces to

$$S_{2\phi}(\omega,\omega')=\sum_{\sigma,\sigma'}\frac{\alpha_{\sigma\sigma'}^2}{2\pi m}\int\int q\,dq\,q'dq'\mathrm{Re}D_\sigma(q,\omega)\mathrm{Re}D_{\sigma'}(q',\omega')\frac{\Theta((2k_F)^2-q^2-(q')^2)}{\pi k_F[(2k_F)^2-q^2-(q')^2]^{1/2}} \ . \tag{27}$$

Making the same substitutions in Eq. (19), for example, with P expressed in terms of δ functions through Eq. (7b), and noting that the q' integral reduces to $\int_0^Q dq'(Q^2-q'^2)^{-1/2}=\pi/2$, Eq. (19) reduces to

$$S_{1\phi}^{(ii)}(\omega)=\sum_{\sigma,\sigma'}\frac{\omega\alpha_{\sigma\sigma'}^2}{\pi m}\int_0^{2k_F}\frac{q^2dq}{2k_F}[\mathrm{Re}D_\sigma(q,\omega)\mathrm{Re}D_{\sigma'}(q,\omega)+\delta_{\sigma\sigma'}(\mathrm{Im}D_\sigma(q,\omega))^2] \ . \tag{28}$$

The diagonal terms [obeying Eq. (18a)] have been added to give the full $S_{1\phi}^{(ii)}$. Comparing Eqs. (27) and (28), only the former (expressing exchange) has nontrivial dependence on q' and ω'; the ω' integral appears in Eq. (21a) relating $S_{2\phi}(\omega,\omega')$ to Im$\Sigma_{2\phi}(\varepsilon,T)$. The analogous integral has already been incorporated in the definition of $S_{1\phi}$ [see Eq. (13)]. This difference in definition accounts for the explicit factor of ω in Eq. (28).

It is useful to proceed with the asymptotic forms of these two functions now, and return to those containing Coulomb interactions later. It is of interest to consider

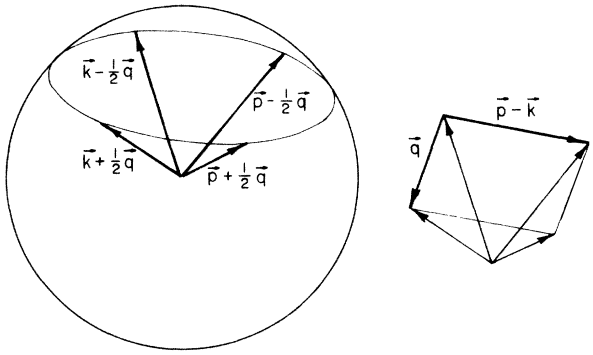

FIG. 8. (a) Four wave vectors on the Fermi surface participating in a momentum-conserving scattering event, and (b) momenta transferred in the direct and exchange contributions [Fig. 7(c)].

the limits of small α and small or large ω. These are obtained in a straightforward manner; recall that phonon propagators with single subscripts denote inverses of diagonal elements of $D^{-1}_{\sigma\sigma'}$ [Eq. (17)], so that with Eq. (25)

$$D_\sigma(q,\omega)=2\omega_{q\sigma}(\omega^2-\omega_{q\sigma}^2-2i\omega\omega_{q\sigma}\alpha_\sigma)^{-1} , \tag{29}$$

where α_σ denotes henceforth a diagonal element of $\alpha_{\sigma\sigma'}$. First, for $\omega \ll \omega_D$, one finds power series in both α and ω, of which the leading terms are

$$S^{(\mathrm{ii})}_{1\phi}(\omega)\cong\frac{4\omega}{\pi m}\sum_{\sigma,\sigma'}\frac{\alpha_\sigma\alpha_{\sigma'}}{c_\sigma c_{\sigma'}}+\frac{\omega^2}{2k_F m}\sum_\sigma\frac{\alpha_\sigma}{c_\sigma^3} , \tag{30a}$$

$$S_{2\phi}(\omega,\omega')\cong\frac{2}{\pi m}\sum_{\sigma,\sigma'}\frac{\alpha_\sigma\alpha_{\sigma'}}{c_\sigma c_{\sigma'}} . \tag{30b}$$

To illustrate the significance of these, the contribution of each to $\mathrm{Im}\Sigma$ is written using Eqs. (13) and (21a); for $\varepsilon=0$ and $T\ll\omega_D$, for example,

$$\mathrm{Im}\Sigma^{(\mathrm{ii})}_{1\phi}(0,T)\cong\frac{12\zeta(2)T^2}{\pi m}\sum_{\sigma,\sigma'}\frac{\alpha_\sigma\alpha_{\sigma'}}{c_\sigma c_{\sigma'}}+\frac{7\zeta(3)T^3}{2k_F m}\sum_\sigma\frac{\alpha_\sigma}{c_\sigma^3} , \tag{31a}$$

$$\mathrm{Im}\Sigma_{2\phi}(0,T)\cong-\frac{6\zeta(2)T^2}{\pi m}\sum_{\sigma,\sigma'}\frac{\alpha_\sigma\alpha_{\sigma'}}{c_\sigma c_{\sigma'}} . \tag{31b}$$

The α^2 terms correspond in all cases to the leading T (or ω) dependences, and may be obtained by evaluating the $D(q,\omega)$ factors at $\omega=0$. These are clearly identified with electron-electron scattering, with $S_{2\phi}$ the exchange counterpart of the α^2 terms in $S^{(\mathrm{ii})}_{1\phi}$. The factor of 2 arises because only parallel spins contribute to $S_{2\phi}$; the factor is precisely 2 only because the Debye-like model leads to purely s-wave electron-electron scattering. Electron–real-phonon processes are represented by the term linear in α, which appears only in $S^{(\mathrm{ii})}_{1\phi}$ and arises from the poles of $|D_\sigma|^2$ (the terms where $\sigma'=\sigma$), with equal contributions from $(\mathrm{Re}D_\sigma)^2$ and $(\mathrm{Im}D_\sigma)^2$. There are also pole contributions to $S_{2\phi}$ and the nondiagonal $S^{(\mathrm{ii})}_{1\phi}$ terms, but these contribute only $O(\alpha^3)$. Furthermore, there are α^3 terms which have been ignored in the approximations (such as dropping $\mathrm{Im}D_\sigma\mathrm{Im}D_{\sigma'}$ from $S_{1\phi}$) of the last section. Such contributions are difficult or impossible to interpret in terms of simple processes.

Corrections to the frequency dependence are more interesting. At low frequencies, the α^2 terms in $S^{(\mathrm{ii})}_{1\phi}$ and $S_{2\phi}$ may be expressed as power series in ω containing odd and even powers, respectively. The term linear in α has purely quadratic ω dependence for $\omega<\omega_D$. In the opposite limit $\omega\gg\omega_D$, only the α^2 terms are present:

$$S^{(\mathrm{ii})}_{1\phi}(\omega)\cong\frac{4(2k_F)^4}{5\pi m\omega^3}\sum_{\sigma,\sigma'}\alpha_\sigma\alpha_{\sigma'}c_\sigma c_{\sigma'} , \tag{32a}$$

$$S_{2\phi}(\omega,\omega')\cong\frac{2(2k_F)^4}{15\pi m\omega^2\omega'^2}\sum_{\sigma,\sigma'}\alpha_\sigma\alpha_{\sigma'}c_\sigma c_{\sigma'} . \tag{32b}$$

Equations (30a) and (32a) show the same asymptotic behavior as Allen and Silberglitt's generalized electron-phonon spectral function $\alpha^2F(\omega)$.[10] The differences are only in detail, primarily in the explicit polarization sums of the present expressions. The double sums, reflecting the nondiagonal character of $\mathrm{Im}D$, are necessary for an accurate treatment of the electron-electron contribution. The exchange contribution [Eq. (32b)] differs from the direct one by more than a factor of 2. This is because the frequency dependence of the effective interaction $g_\sigma D_\sigma g_\sigma$ is important at all but the lowest frequencies.

The precise nature of the high-frequency tails in Eqs. (32a) and (32b) is unimportant for $\mathrm{Im}\Sigma$. What matters is that these phonon-mediated contributions cut off for $\omega>\omega_D$, if less abruptly than the real-phonon contribution. Because of this, the decay rate contributions from real- and virtual-phonon processes are all linear in T for $T\gg\omega_D$, so that here real phonons dominate with $\mathrm{Im}\Sigma_{1\phi}(0,T)\sim\alpha T$, while $\mathrm{Im}\Sigma_{2\phi}(0,T)\sim-\alpha^2T$.

The remarks above do not apply to the Coulomb interaction, which produces a (sometimes observable[21]) quadratic temperature dependence at high as well as low temperatures. To illustrate these effects, consider the remaining spectral functions assuming, for simplicity, a momentum- and spin-independent scattering amplitude V_c. The momentum sums in Eqs. (14) and (20) are again done with the help of Eq. (26). The resulting expressions are simplified by collecting some factors in Eq. (26) together with V_c as follows:

$$\frac{m^2}{2\pi^2\hbar^3}V_c=\frac{N_0}{v_F}V_c=\frac{\mu_c}{v_F} , \tag{33}$$

where μ_c is the usual Coulomb pseudopotential, N_0 the density of states per spin, and v_F the Fermi velocity. The resulting spectral functions are

$$S^{(\mathrm{i})}_{1\phi}(\omega)\cong\frac{\omega\mu_c}{mv_F}\sum_\sigma\frac{\alpha_\sigma}{c_\sigma}\quad(\omega\ll\omega_D) , \tag{34a}$$

$$S_c(\omega)=\frac{\pi\omega\mu_c^2}{2mv_F^2}\quad(\text{all }\omega) . \tag{34b}$$

Regarding μ_c/v_F and α_σ/c_σ as the same order, it is clear that these expressions are comparable with the α^2 terms found earlier. Expression (34b) is valid for the

whole frequency range of interest here, while (34a) is just the leading term in a series of odd powers of ω. The additional contribution to (34a) from the pole of D is of order $(\mu_c/v_F)(\alpha_\sigma/c_\sigma)^2\omega^2$, which is negligible. For $\omega \gg \omega_D$ the asymptotic form is

$$S_{1\phi}^{(i)}(\omega) \cong \frac{2\mu_c(2k_F)^2}{3mv_F\omega} \sum_\sigma \alpha_\sigma c_\sigma \quad (\omega \gg \omega_D) . \tag{35}$$

This and Eq. (34b) show that the only significant electron-electron contribution to $\mathrm{Im}\Sigma$ at high temperatures comes from $S_c(\omega)$. Combining this S_c contribution with the electron-phonon contribution contained in $S_{1\phi}^{(ii)}$, one finds

$$\mathrm{Im}\Sigma(0,T) \cong \frac{3\pi\zeta(2)\mu_c^2}{2mv_F^2} T^2 + \pi\lambda T \quad (T \gg \omega_D) , \tag{36}$$

where λ is the usual electron-phonon interaction parameter, related linearly to the phonon linewidths.[22] In the present model the precise relation is

$$\lambda = Z - 1 = \frac{2v_F}{\pi} \sum_\sigma \frac{\alpha_\sigma}{c_\sigma} . \tag{37}$$

This relation is useful in the limit $T \ll \omega_D$. Here, there are electron-electron contributions (terms of order α^2 or the equivalent) from each of $S_{1\phi}$ [(i), (ii), and (iii)], $S_{2\phi}$, and S_c. Their leading ω (ω') dependences are found in Eqs. (30) and (34), and the resulting leading temperature dependences [all $\sim T^2$ as in Eqs. (31)] form a perfect square. Adding to this the electron-phonon contribution in Eq. (31a), the result is

$$\mathrm{Im}\Sigma(0,T) \cong \frac{3\pi\zeta(2)}{2mv_F^2}(\lambda - \mu_c)^2 T^2 + \frac{7\zeta(3)}{2k_F m} \sum_\sigma \frac{\alpha_\sigma}{c_\sigma^3} T^3 \quad (T \ll \omega_D) . \tag{38}$$

An electron-electron contribution of this simplicity occurs only if the scattering amplitude is isotropic, and only in the leading (quadratic) temperature or energy dependences, which do not reflect the energy dependence of the phonon-mediated interaction. The electron-phonon contribution to Eq. (38) can be written in terms of λ if polarization differences are ignored, in which case it is $\sim \lambda T^3/\omega_D^2$.

As Allen and Silberglitt have pointed out,[10] the electron-electron contribution dominates at very low temperatures, $T < \alpha\omega_D$, and they have estimated α in the range 10^{-3}–10^{-2} for typical elementary metals. At high temperatures $T \sim \omega_D$ the electron-electron contribution is a small fraction $\mu_c c_\sigma/v_F \sim \alpha$ of the electron-phonon one, but may sometimes be observable in the T dependence of the Lorenz ratio.[21]

IV. CONCLUSIONS

The simplifying model used in the last section illustrates the most important qualitative features of the spectral functions and the decay rate through simple, transparent, and probably not very accurate expressions. Perhaps it is worthwhile to briefly reconsider these features in more general terms. First, the particle-hole decay mode (due to the Coulomb and virtual-phonon-mediated interactions) is represented by all three self-energy diagrams, Figs. 1(a)–1(c), and depends quadratically on the phonon linewidth parameter α [Eq. (23)] and the effective Coulomb interaction potential V_c [Eqs. (22)]. The emission and absorption of real phonons are accounted for by just that part of Fig. 1(b) [shown in Fig. 5(ii)] in which the phonon line is cut into the two similar polarization components $\sigma = \sigma'$. Real- and virtual-phonon processes contributed by this piece are distinguished by linear and quadratic dependences on α, respectively. According to Fig. 7 the particle-hole decay mode may be represented alternatively by an effective electron-electron interaction potential

$$u = \sum_\sigma g_\sigma \mathrm{Re}D_\sigma g_\sigma + V_c .$$

It is understood in this context that D is a function of a real frequency variable. The corresponding scattering amplitude [as in Eqs. (22)] depends upon wave vector, spin, and (because of exchange) two frequency variables. This amplitude leads to a decay rate either through a spectral function of the form $S(\omega,\omega')$ and Eq. (21a), or directly from the Fermi golden rule as applied to electron-electron scattering. As noted in Sec. III, this decay rate includes not only the full electron-electron contribution, but also half the electron-phonon contribution; the remaining half is provided by the appropriately averaged scattering probability $\sum_\sigma |g_\sigma|^2 (\mathrm{Im}D_\sigma)^2$.

At a small cost, a more concise prescription can be given: The full electron-phonon and electron-electron contributions are produced together by using the complex electron-electron interaction potential

$$\tilde{u} = \sum_\sigma g_\sigma D_\sigma g_\sigma + V_c ,$$

which must be paired with its complex conjugate when used in Fig. 7. Clearly this prescription adds the desired term, but it also adds errors to $\mathrm{Im}\Sigma_{2\phi}$ and to the off-diagonal components of $\mathrm{Im}\Sigma_{1\phi}$. These errors include the familiar type $O(\alpha^3)$ that are inherent in the formalism, plus new errors $O(\alpha^2\omega^2)$ for $\omega < \omega_D$. These may be ignored because the combined α and ω dependences make them negligible compared with the electron-phonon contribution over the entire frequency range.

Incidentally, the parameters α and V_c are related to the vertex functions g_σ and Γ, by Eqs. (24b) and (25) and Eqs. (22a) and (22b), respectively. That only the physical vertex functions appear in the quasiparticle and phonon decay rates was established in Sec. II.

The general frequency dependence can be discussed by formally decomposing the spectral function according to real-phonon and particle-hole pair contributions, say $S_\phi(\omega)$ and $S_{p\text{-}h}(\omega,\omega')$, as distinguished above. $S_\phi(\omega)$ is to be used in Eq. (13) and $S_{p\text{-}h}(\omega,\omega')$ in Eq. (21a). $S_\phi(\omega)$ is equivalent to the usual $\alpha^2F(\omega)$, whose qualitative behavior is well known: It is initially quadratic in ω, has sharp structure at higher frequencies reflecting structure in the phonon density of states, the Fermi surface, and the matrix elements g, and then vanishes for $\omega > \omega_D$.

The particle-hole pair function $S_{p\text{-}h}(\omega,\omega')$ is initially constant, exhibits relatively weak structure at intermediate frequencies, and finally approaches algebraically a different constant (characteristic of purely Coulomb scattering) for $\omega > \omega_D$. If a single-variable particle-hole spectral function were defined by performing the ω' integral, then this function would be linear in ω for $\omega \ll \omega_D$ and $\omega > \omega_D$, but the crossover at intermediate frequencies would be temperature dependent. Relatively little structure is expected in $S_{p\text{-}h}$ because contributions in the momentum integrals are distributed throughout the Brillouin zone, rather than being concentrated near the poles of D as they are in the case of $S_\phi(\omega)$.

In the superconducting phase, while $S_\phi(\omega)$ [the usual $\alpha^2F(\omega)$] is not changed from the normal phase, $S_{p\text{-}h}(\omega,\omega')$ exhibits structure associated with the gap in the quasiparticle spectrum, which carries through to the decay rate. This will be the subject of a future publication.

---

*Present address: Department of Physics, Indiana University of Pennsylvania, Indiana, PA 15705.

[1]A. B. Migdal, Zh. Eksp. Teor. Fiz. **34**, 1438 (1958) [Sov. Phys.—JETP **7**, 996 (1958)].

[2]Y. Nambu, Phys. Rev. **117**, 648 (1960).

[3]G. M. Eliashberg, Zh. Eksp. Teor. Fiz. **38**, 966 (1960) [Sov. Phys.—JETP **11**, 696 (1960)].

[4]D. J. Scalapino, J. R. Schrieffer, and J. W. Wilkins, Phys. Rev. **148**, 263 (1966).

[5]E. G. Batyev and V. L. Pokrovskii, Zh. Eksp. Teor. Fiz. **46**, 262 (1964) [Sov. Phys.—JETP **19**, 181 (1964)].

[6]S. B. Kaplan, C. C. Chi, D. N. Langenberg, J. J. Chang, S. Jafarey, and D. J. Scalapino, Phys. Rev. B **14**, 4854 (1976).

[7]Examples showing a range of approaches are A. H. MacDonald, R. Taylor, and D. J. W. Geldart, Phys. Rev. B **23**, 2718 (1981); A. H. MacDonald and D. J. W. Geldart, J. Phys. F **10**, 677 (1980); C. A. Kukkonen and J. W. Wilkins, Phys. Rev. B **19**, 6075 (1979); C. A. Kukkonen and A. W. Overhauser, *ibid.* **20**, 550 (1979).

[8]C. A. Kukkonen and A. W. Overhauser, Phys. Rev. B **20**, 550 (1979).

[9]T. Holstein, Ann. Phys. (N.Y.) **29**, 410 (1964).

[10]P. B. Allen and R. Silberglitt, Phys. Rev. B **9**, 4733 (1974).

[11]J. M. B. Lopes dos Santos and D. Sherrington, J. Phys. F **13**, 1233 (1983).

[12]J. M. B. Lopes dos Santos and D. Sherrington, J. Phys. F **14**, 2039 (1984).

[13]J. S. Langer, Phys. Rev. **124**, 997 (1961).

[14]K. Schwartzman and W. E. Lawrence, in *Proceedings of the 17th International Conference on Low Temperature Physics,* edited by U. Eckern, A. Schmid, W. Weber, and H. Wuhl (North-Holland, Amsterdam, 1984), Vol. II, p. 1055.

[15]R. Kobes and G. Semenoff, Phys. Rev. B **34**, 4338 (1986).

[16]See, for example, B. K. Bhattacharyya and J. C. Swihart, Phys. Rev. B **30**, 1656 (1984); J. Phys. F **14**, 1651 (1984).

[17]P. Nozieres, *Interacting Fermi Systems* (Benjamin, New York, 1964).

[18]K. Schwartzman, Bull. Am. Phys. Soc. **31**, 1002 (1986).

[19]Frequency dependence of the real part occurs on the scale of prominent features in the band structure, and is therefore negligible for our purposes. The same statement applies to deviations from the linear frequency dependence of the imaginary part.

[20]P. B. Allen, Phys. Rev. B **6**, 2577 (1972).

[21]M. J. Laubitz, Phys. Rev. B **2**, 2252 (1970).

[22]See Eq. (12) of Ref. 20.